Indian Ocean Low Clouds during the Winter Monsoon

SANDRINE BONY

Laboratoire de Météorologie Dynamique du CNRS, Paris, France

WILLIAM D. COLLINS AND DAVID W. FILLMORE

Climate and Global Dynamics Division, National Center for Atmospheric Research, Boulder, Colorado*

(Manuscript received 12 January 1999, in final form 22 June 1999)

ABSTRACT

While low-level clouds over the Pacific and Atlantic Oceans have been investigated extensively, low clouds over the Indian Ocean are not as well characterized. This study examines the occurrence of nonoverlapped low clouds over the Indian Ocean during the northeast monsoon using several sources of data. Climatologies derived from surface observations and from the International Satellite Cloud Climatology Project are reviewed. Another cloud climatology is developed using infrared and visible imagery from the Indian geostationary satellite. The new climatology has better spatial and temporal resolution than in situ observations. The three datasets are generally consistent and show several persistent features in the cloud distribution. During January–April, maxima in the occurrence of low clouds occur at subtropical latitudes over the Arabian Sea, the Bay of Bengal, the China Sea, and the southern Indian Ocean. The predominant types of low clouds differ in the northern and southern areas of the Indian Ocean region and China Sea. The Arabian Sea and the Bay of Bengal are covered mostly by cumulus clouds, while the southern Indian Ocean and the China Sea are covered mostly by large-scale stratiform clouds such as stratocumulus. These observations are consistent with atmospheric analyses of temperature, humidity, and stability over the Indian Ocean.

1. Introduction

Marine low-level clouds are characterized by a high albedo relative to the ocean surface and a cloud-top temperature close to the sea surface temperature. It follows from these characteristics that low clouds exert a large negative cloud radiative forcing (Hartmann et al. 1992) and impose significant changes on the surface and planetary radiation budgets. Moreover, the cloud-top albedos of these clouds fall in the range of albedos that exhibit maximum sensitivity to a change in the cloud droplet concentration (Schwarz and Slingo 1996). Marine low clouds are thought to be the principal clouds susceptible to influence by natural or anthropogenic aerosols. Thus these clouds are likely to play a critical role in the long-term evolution of the earth radiation budget. A quantitative assessment of the climate impacts requires information on where and when low-level clouds occur over the global ocean and determination of the factors that control the formation, type, and radiative properties of low clouds. This information is also necessary to improve the ad hoc numerical parameterizations of these clouds in climate models (e.g., Mechoso et al. 1995).

Marine low clouds have been extensively investigated over the Pacific and Atlantic Oceans (e.g., Hanson 1991; Klein and Hartmann 1993; Klein 1997; Norris 1998a), but relatively few studies have focused on the Indian Ocean. Information on the distribution of low clouds over the Indian Ocean is required for investigations of ocean–atmosphere interactions over this crucial part of the global ocean and for studies of the indirect effect of aerosols. The Indian Ocean is surrounded by nations with rapidly increasing emissions of sulphates and many types of anthropogenic aerosols (Wolf and Hidy 1997). These emissions may interact with clouds and affect the climate through direct and indirect radiative forcing. During the winter monsoon in January–April, the predominant circulation over the northern Indian Ocean consists of a low-level flow from the northeast and two anticyclones at subtropical latitudes (Krishnamurti et al. 1997a). The meteorological conditions during the winter monsoon support large-scale transport of aerosols from the Indian subcontinent toward ocean regions presumably covered by low clouds (Krishnamurti et al. 1997b).

* The National Center for Atmospheric Research is sponsored by the National Science Foundation.

Corresponding author address: Dr. William D. Collins, NCAR/CGD, P.O. Box 3000, Boulder, CO 80307-3000.
E-mail: wcollins@ucar.edu

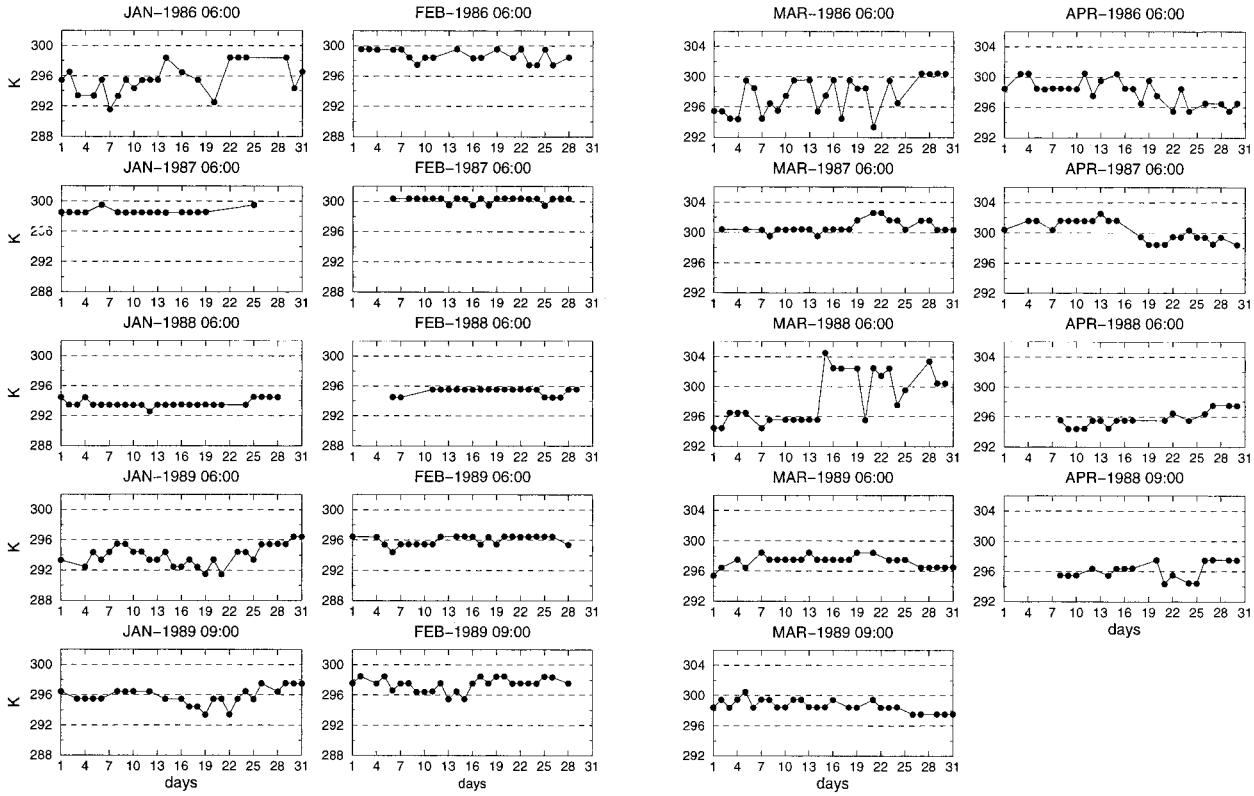

FIG. 1. Time variation of the 10th percentile value of the INSAT IR brightness temperature over the Indian Ocean computed from daily image radiance distributions.

These conditions are favorable for observational investigations of the indirect effect of aerosols. Apart from enhancing existing climatologies of low-cloud distribution, this study is also intended to support field experiments in the Indian Ocean region such as the Indian Ocean Experiment (INDOEX). One of the primary scientific objectives of INDOEX is to quantify the indirect effects of aerosols on low-cloud systems over space scales and timescales relevant for climate models (Ramanathan et al. 1996).

So far, our knowledge about Indian Ocean low clouds is derived from ship-based observations (e.g., Warren et al. 1988). Such in situ observations are suitable for constructing long-term climatologies, but they are difficult to synthesize with other remotely sensed quantities such as aerosol optical depth or liquid water path because ship observations in remote areas of the Indian Ocean are very infrequent. The need to create a ''dense'' dataset for the Indian Ocean is one of the primary motivations for this study. We will focus on nonoverlapped marine low clouds that occur during daytime.[1] By definition, satellite measurements of radiation from these cloud systems are not affected by higher-altitude clouds. The distribution of nonoverlapped low clouds is particularly important because the top-of-atmosphere shortwave cloud radiative forcing of low-level clouds is maximized when these clouds are not shielded by upper-level cloud systems. In addition, geographical gradients detected in the shortwave radiation are linked unambiguously to gradients in the low-cloud field. In studies of the INDOEX data, information concerning the distribution and physical properties of Indian Ocean low clouds will be used to understand the climatological context of aircraft and ship observations. Also, satellite data on low-cloud systems will be used to extrapolate in situ observations to larger regions.

In this paper, we review existing climatologies of marine low clouds over the Indian Ocean during the winter monsoon. In particular, we consider the surface cloud dataset produced by Hahn et al. (1996) and the database from the International Satellite Cloud Climatology Project (ISCCP; Rossow and Schiffer 1991). However, those two climatologies suffer from some shortcomings over the Indian Ocean. The quality of ISCCP data is adversely affected by the gap in geosynchronous satellite coverage over the central Indian Ocean (Rossow and Garder 1993). Surface observations of marine clouds are sparse and infrequent due to the small number of shipping routes in this region. We add to the information provided by those two datasets by investigating

[1] Throughout this study, the term ''low clouds'' should be understood to mean nonoverlapped low clouds.

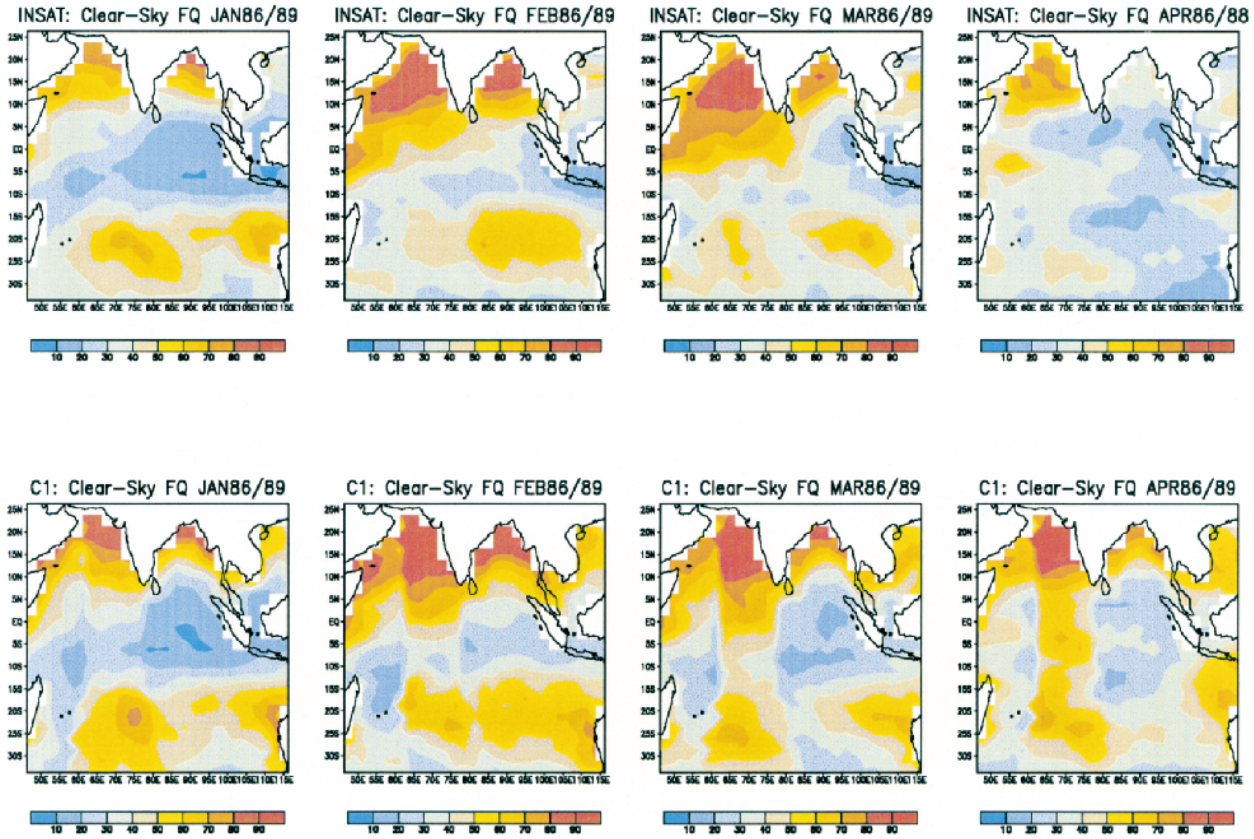

FIG. 2. Monthly percentage of clear-sky pixels within 2.5° × 2.5° regions during 1986–89 derived from (top) INSAT data and (bottom) ISCCP/C1 data at 0600 and 0900 UTC times using the IR clear-sky composite procedure.

marine low clouds using the Indian geostationary satellite (INSAT). The methodologies used to detect low clouds from ISCCP and surface observations are presented in section 2, and the analysis method for INSAT data is presented in section 3. The frequency of occurrence and the amount when present of nonoverlapped low clouds derived from the three datasets are compared in section 4. In section 5, we discuss the different types of low clouds over the Indian Ocean and the relationship of these clouds to meteorological indexes derived from the European Centre for Medium-Range Weather Forecasts (ECMWF) reanalysis. This section is intended to evaluate the consistency of our results with meteorological conditions rather than evaluate the conditions required to form low-level clouds. A summary and concluding remarks are presented in section 6.

2. Surface observations and the ISCCP/C1 dataset

a. Surface observations

The dataset produced by Hahn et al. (1996) is used to investigate surface observations of low clouds over the Indian Ocean. It includes instantaneous ship and station observations of cloud types and weather during 1982–91. Since each report has been put through a series of quality and consistency control checks, no further quality checking is done in this study. Only reports that satisfy the illumination criteria for reliable cloud detection (Hahn et al. 1996) and that correspond to local times in the INSAT dataset are included. The surface observers also classify the observations of cloud amount by cloud type (Norris 1998a). The distribution of cloud types obtained from surface data is discussed in section 4.

In this analysis, ''nonoverlapped low-level clouds'' (NOLC) refer to the low-level clouds that do not occur simultaneously with higher-level clouds. The frequency of occurrence of NOLC is computed in regions of 2.5° × 2.5° as the percentage of days in each month during which all reports indicate the presence of nonoverlapped stratocumulus or cumulus clouds. The cloud amount when present (AWP) is computed by averaging the low-cloud amount from the reports of NOLC. The angular size of the regions will be held fixed at 2.5° in latitude and longitude unless otherwise noted. Alternate methods for accounting for the clear-sky bias (Hahn et al. 1996) proposed by Norris (1998b) can increase the frequency and AWP by between 0% and 8% relative to the values reported here. The increases are largest in the southern Arabian Sea and southeastern Indian Ocean.

Surface observations over the Indian Ocean are rel-

atively sparse. Data are concentrated in the Northern Hemisphere along a few ship routes, most of them bordering the Saudi Arabian region or the western coast of India and crossing the Gulf of Bengal up to Malaysia and China. When considering all synoptic hours of observations during January–April 1982–91 that coincide with ISCCP dayside images, the monthly average number of available reports is less than 2 yr^{-1} in about 60% of the regions of the Indian Ocean. It is larger than 10 in only 10% of the regions (not shown). If the requirement of coincidence with available INSAT dayside imagery is relaxed, the number of observations increases by approximately 2.5 times. However, the frequency of occurrence and AWP of NOLC obtained with the larger dataset are very similar to the values obtained with the subset of surface observations used here.

b. ISCCP/C1 data

The ISCCP algorithm uses infrared and visible imagery from several operational meteorological satellites to retrieve cloud properties including cloud amount and cloud type (Rossow and Schiffer 1991). The original satellite radiance data represent measurements over fields of view ranging from 4 to 8 km in size. The data are sampled to a resolution of about 25–30 km. The cloud detection algorithm consists of a two-stage process. Clear-sky radiance values are first estimated by analyzing the radiance data over several spatial and temporal domains. Individual pixels are then classified as clear or cloudy depending on the difference between the pixel radiance and the local clear-sky radiance estimate (Rossow et al. 1991). Then a radiative transfer model is used together with atmospheric profiles of temperature, water vapor, and ozone derived from the Television Infrared Observational Satellite (Tiros) Operational Vertical Sounder to determine the cloud altitude and the cloud optical thickness associated with each individual cloudy pixel. In this study, we use daytime data derived from the ISCCP/C1 dataset. It includes the number of clear-sky and cloudy pixels in different classes corresponding to different ranges of cloud-top pressure and cloud optical thickness every 3 h for regions of approximately 280 km $\times$ 280 km. Low-level clouds with an optical thickness greater (smaller) than 3.6 are classified as stratocumulus (cumulus, respectively).

For each region, we compute the monthly frequency of occurrence of NOLC as the percentage of days in each month for which the number of low-cloud pixels in the region is greater than zero and equals the number of cloudy pixels. The ISCCP retrieval algorithm includes the assumption of nonoverlapped clouds at the pixel level. The derivation of NOLC from ISCCP ensures consistency with the derivation of NOLC from INSAT, which is based upon aggregate statistics over an entire region (section 3c). The cloud AWP of NOLC is computed as the ratio of the number of nonoverlapped low-cloud pixels over the total number of pixels. Note that the detection of low-level clouds from satellites is complicated, or even impossible, when higher-level clouds occur simultaneously. This does not affect the present study since the analysis is focused on nonoverlapped low clouds.

The reliability of ISCCP data over the Indian Ocean is affected by the lack of continuous satellite measurements. Data from INSAT were not available during the processing of ISCCP/C1 data. The cloud products over the western and eastern sides of the Indian Ocean are therefore derived from imagery from the Meteorology Satellite (Meteosat) and the Japanese Geostationary Meteorological Satellite (GMS), respectively. Between 60° and 80°E, data from these geostationary satellite are significantly degraded by the viewing geometry and are therefore not included in the ISCCP dataset. The gap in the measurements is partially filled using data from the advanced very high resolution radiometer (AVHRR) on polar orbiters operated by the National Oceanic and Atmospheric Administration. However, the AVHRR data are available only twice daily at tropical latitudes. The incomplete diurnal sampling causes strong discontinuities in the ISCCP products around 60° and 80°E and introduces systematic errors in cloud properties between these longitudes.

3. Analysis of INSAT observations

a. INSAT data

Because of the artifacts in the ISCCP data and the coarse geographical coverage of surface cloud observations, there is a need for complementary dense and continuous information about the cloud systems over the Indian Ocean. We investigate nonoverlapped low-cloud systems using data from the Indian National Satellite System INSAT that were made available to the scientific community a few years ago.

INSAT was developed by the Indian Space Research Organization to provide, among other services, data in support of meteorological applications within the Indian Meteorological Department (IMD). The *INSAT-1B* satellite is a three-axis stabilized satellite operated in geostationary orbit with a subsatellite longitude of 74.5°E since September 1983. The radiances measured by an imaging instrument, the very high resolution radiometer, are derived from visible (0.55–0.75 μm) and infrared (10.5–12.5 μm) narrowband channels with a nadir resolution of 2.75 and 11 km, respectively. The limited INSAT dataset provided by the National Center for Atmospheric Research and the IMD consists of reduced resolution full-disk images. The INSAT pixel data are sampled every 22 km approximately at nadir (Smith et al. 1989), and the visible radiances are divided by the cosine of the local solar zenith angle. The Indian Ocean is totally illuminated at 0600 and 0900 UTC synoptic hours. While INSAT data at 0600 UTC are available

for January 1986–March 1989, data at 0900 UTC are available for April 1988–March 1989 only.

Two kinds of quality checks have been applied to the data. First, the visible images have been inspected manually, and images that contain invalid scan lines or missing segments have been eliminated. Second, spurious variations in the infrared (IR) radiances related to orbital changes in the satellite operating environment have been identified, and the corresponding images have been omitted from further analysis. For that purpose we inspect, following Desormeaux et al. (1993), the time evolution of the 10th percentile of INSAT IR brightness temperatures (IRBT) computed from individual image radiance distributions (Fig. 1). The standard deviation of this quantity over a month is generally less than 1 K, and we reject from the study the months for which it is larger than 1.5 K. This criterion eliminates data from January 1986, March 1986, and March 1988. The large variations in the 10% percentile IRBT are associated with changes in the sun–satellite orientation that apparently affect the temperatures of the IR radiometer and blackbody calibration systems on board INSAT. This thermal effect is known to be exacerbated during the equinox season (e.g., March), as the geostationary satellite passes in and out of the earth's shadow near local midnight.

Tiernego (1996) showed that at high temperatures (around 295 K), the INSAT IRBT are 2–5 K lower than coincident AVHRR clear-sky scenes, and that at colder temperatures, the brightness temperatures are comparable to within 1–2 K. To facilitate the comparison at different stages of this study between INSAT and ISCCP/C1 data, we use the time-varying normalization coefficients proposed by Rossow et al. (1992) to provide an absolute calibration to INSAT IR radiances. The normalization was derived by relating INSAT radiances to coincident GMS radiances and then applying an empirical correction to GMS based upon the AVHRR instrument.

Our detection of low clouds using INSAT is made in two steps. First, we determine whether each individual INSAT pixel is clear or cloudy by following a procedure very similar to the infrared clear-sky composite algorithm used in ISCCP/C1. Then, we identify regions covered by NOLC by analyzing the spatial variability of visible (VIS) and IR radiances, and we compute the AWP from the fraction of clear-sky pixels determined in the first step.

b. Determination of clear-sky IR radiances

INSAT clear-sky infrared radiances for ocean scenes are determined using a procedure quite similar to that used in ISCCP and presented by Rossow et al. (1991). First, the spatial variability of the IR radiances is analyzed within each region, and all pixels determined to be colder than the warmest pixel by 3.5 K are labeled ''cloudy.'' Next, the time variability of the IR radiances over three days at the same UTC is determined at the resolution of the original images (about 22 km). All pixels determined to be colder by 3.5 K than the values on the previous or following day are labeled ''cloudy,'' and pixels having a temperature differing by less than 1.1 K from values on the previous or following day are labeled ''clear.'' The remaining pixels are labeled ''undecided.'' When the test result for one direction in time is in strong conflict with the result for the other direction in time, the pixel is labeled ''mixed.'' Note that for this second test, the radiance images have been corrected for effects of viewing geometry using the ISCCP limb-darkening functions for clear-sky IR radiances. Then, the test results based on space and time variabilities are combined to yield a final classification for each pixel. The final label is that determined from the time test with the exception of two cases. When the time test label is ''undecided'' or ''clear'' and the space test label is ''cloudy,'' the final label is ''cloudy'' (in the first case) or ''mixed'' (in the second case).

Statistics are calculated for spatial domains of 0.625° × 0.625° (about 70 km) for a long-term period of 30 days and for a short-term period of 15 days. Based on the number of clear-sky pixels and on the average and maximum IR brightness temperatures in each domain of 0.625°, the ISCCP infrared clear-sky composite logic is used to determine the clear-sky IR radiance value in each 0.625° region for each 15-day period. The different threshold values involved in this logic are similar to that used for the ISCCP/C1 stage data. Finally, pixels with an infrared radiance colder by more than 2.5 K than the 15-day clear-sky value are classified as cloudy.

The percentage of clear-sky pixels derived from INSAT data for January–April 1986–89 is generally in good agreement with that derived from ISCCP/C1 data using the IR clear-sky composite procedure (Fig. 2). The clear-sky percentage in each region is defined as the number of clear-sky pixels divided by the total number of pixels for each month. Nevertheless, some discrepancies between the two datasets are apparent. The discrepancies may arise from a combination of factors, including differences in temporal sampling, the size of the infrared pixels, and the viewing geometry of the satellites. The INSAT infrared dataset is not continuous in time, and the nadir resolution of the INSAT imager is lower than the resolution of the Meteosat and GMS instruments. The lower resolution increases the chances of cloud contamination in a given pixel. The largest discrepancies between INSAT and ISCCP occur between 60° and 80°E, where gaps in geosynchronous satellite coverage introduce artificial discontinuities in ISCCP data. In this sector, the clear-sky frequency derived from ISCCP/C1 is generally larger than in the adjacent Meteosat or GMS sectors. INSAT data suggest this feature is not representative of the actual geographical variability, especially in the Northern Hemisphere.

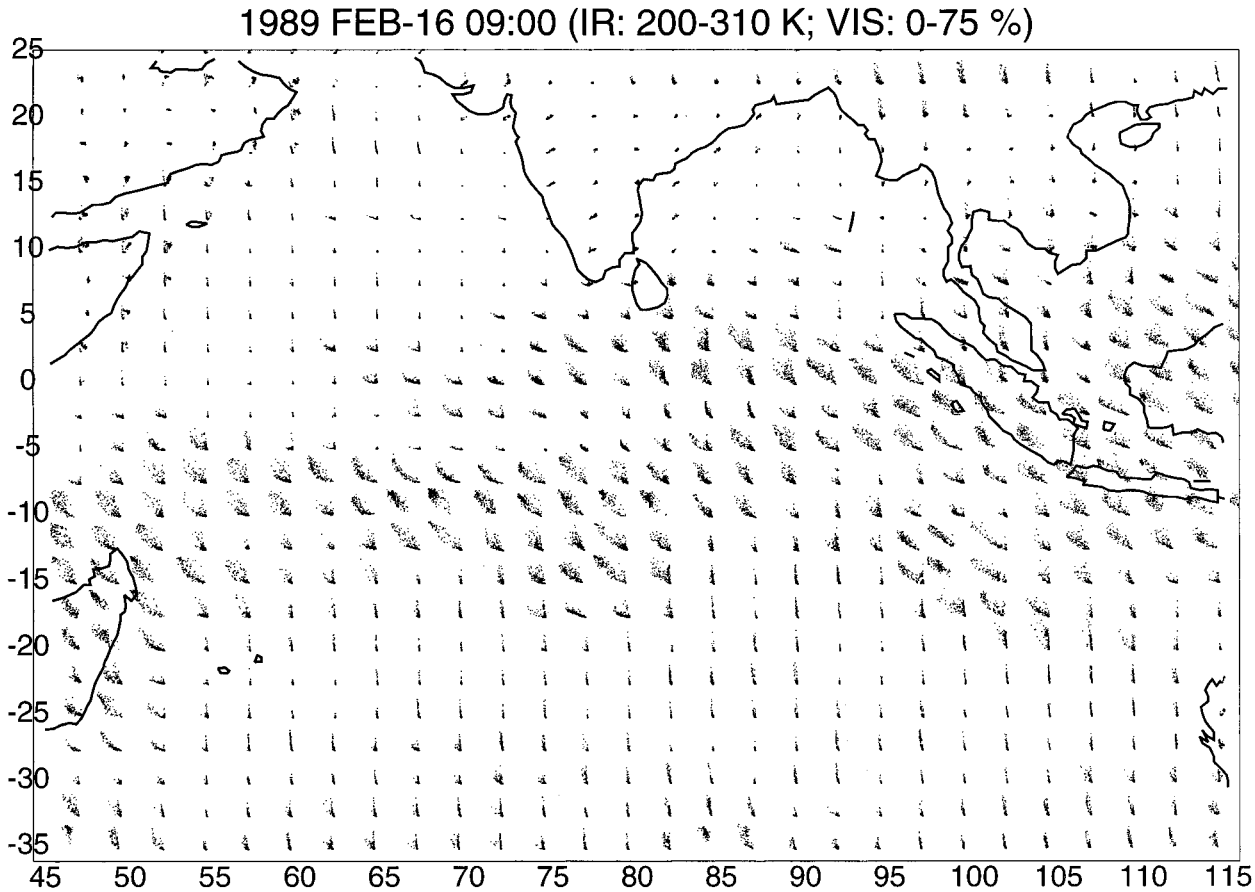

FIG. 3. Geographic distribution of 2.5° × 2.5° visible–infrared radiance diagrams derived from instantaneous INSAT images on 16 Feb 1989 at 0900 UTC. The abscissa and ordinate correspond to infrared–visible axis, respectively. The axis limits are 200–310 K for the IR brightness temperature and 0%–75% for the visible reflectance.

Eastward of about 105°E, clear-sky frequencies derived from INSAT are systematically smaller than corresponding ISCCP values. This is presumably related to the large viewing angles of the INSAT satellite over this region and to insufficient correction of limb-darkening effects at such angles. Finally, we note that in April, INSAT data exhibit smaller clear-sky frequencies than ISCCP. The relatively large number of missing INSAT images during this month is likely to affect the statistical determination of IR clear-sky radiances and may partly explain this difference.

c. Identification of nonoverlapped low clouds

It has long been recognized from experimental (Coakley and Baldwin 1984; Desbois and Sèze 1984; Sèze and Rossow 1991) and theoretical (Platt 1983; Arking and Childs 1985) studies that the relative spatial variability of infrared and visible radiances on the mesoscale is a good indicator of the type of cloud systems present. As illustrated by Fig. 3, the shape and the orientation of the VIS–IR scatterplot diagrams for 2.5° regions reveal different climatic regimes.[2] The intertropical convergence zone (ITCZ), associated with multilayered convective clouds or mixtures of different cloud types, is characterized by a large variability of both the visible and infrared radiances. Clear-sky regions such as those found over desert areas are characterized by a weak variability of both the visible and infrared radiances. The presence of optically thin or broken cirrus, apparent over the Arabian Sea and in the vicinity of the ITCZ in Fig. 3, is associated with large variations in the infrared radiances with small variations in the visible reflectance. Low-cloud systems such as those found at subtropical latitudes are characterized by a weak variability of the infrared brightness temperature and by a large variability of the visible reflectance. The bispectral characteristics of low-cloud systems are due to a combination of factors including partial cloud cover, scattering from small-scale features such as domes, and the variability of the in-cloud liquid water content (Cahalan et al. 1994).

Our identification of regions covered by NOLC sys-

[2] A 2.5° × 2.5° region contains between 60 and 160 INSAT pixels.

tems consists of identifying areas with relatively low variability in the infrared radiances and relatively large variability in the visible reflectances.[3] The orientation of the VIS–IR distribution is characterized for each ocean region by an angle Θ defined by $\Theta = \arctan(S)$. The slope S is the linear regression coefficient of the least squares fit to $\mathrm{VIS} = S\mathrm{IR} + \mathrm{VIS}_o$ computed by $S = \mathrm{Cov}(\mathrm{VIS}, \mathrm{IR})/\sigma^2(\mathrm{IR})$, and VIS_o is an intercept. Visual inspection of the shape of various VIS–IR distributions suggests identifying NOLC with regions where $\sigma(\mathrm{IR}) < 3$ K and $\Theta < \Theta_0 = -55°$. However, in regions of low amounts of cloud cover, the VIS–IR slope S may be less than in regions of high amounts of cloud cover because the cloud infrared emissivity is not unity. To a first order of approximation, we take this fact into account by choosing the same $\sigma(\mathrm{IR})$ threshold but a lower Θ threshold, $\Theta_0 = -45°$, in regions where the cloud cover is less than 50%.

In order to assess this simple methodology of low-clouds detection using INSAT radiances, the identification criteria for NOLC have been analyzed using coincident retrievals of NOLC from ISCCP. The comparison is performed for ocean regions between 45° and 55°E and 85° and 95°E during February 1986–89. The latitude is restricted to 35°S–25°N. The distribution of Θ and $\sigma(\mathrm{IR})$ derived from INSAT imagery has been stratified according to the ISCCP cloud classification (Fig. 4). More than 95% of the regions classified by ISCCP as covered by NOLC are associated with an INSAT $\sigma(\mathrm{IR})$ less than 3 K (not shown). Although the distribution of Θ values obtained by considering all cloudy regions is bimodal, it is unimodal when it is restricted to regions where low-level clouds represent more than 95% of the total cloud cover. In accordance with our choice of Θ_0 values, we find that most Θ values associated with nonoverlapped low clouds are smaller than Θ_0. However, the Θ distribution obtained for low-cloud regions is less narrow for AWP <50% than for AWP >50%. This suggests that for AWP <50%, quantitative differences between INSAT and ISCCP/C1 estimates of the NOLC occurrence may be related to the choice of the Θ_0 value. Despite the uncertainty in the Θ_0 value for AWP <50%, ISCCP data suggest that regions satisfying the Θ_0 and $\sigma(\mathrm{IR})$ criteria are predominantly covered by low-level clouds.

Examination of the INSAT IRBT reinforces this conclusion. For the same two bands of longitude (45°–55°E and 85°–95°E), we have compared the distributions of the 2.5° average INSAT IR radiance values classified as NOLC by the INSAT and ISCCP algorithms. The distributions in these two regions are quite similar (Fig. 5a). However, the INSAT IRBT in low-cloud regions determined by our method is colder by 2 K on average than the IRBT obtained by using the ISCCP retrieval. This discrepancy slightly increases as the low-cloud amount increases (Fig. 5b). Compared to the ISCCP algorithm for which the low-cloud top pressure is higher than 680 hPa by definition (section 2b), the INSAT detection method is thus likely to identify low clouds with higher top altitude. In 20% of the low-cloud regions classified by INSAT, the ISCCP cloud-top pressure is smaller than 680 hPa (not shown). The simple detection method using INSAT data is thus likely to report larger frequencies of regions covered by NOLC than the ISCCP algorithm, especially in regions of large cloud amount. Note that in NOLC regions identified by ISCCP, the mean IRBT derived from INSAT radiances is higher by about 2 K than that derived from ISCCP (i.e., from

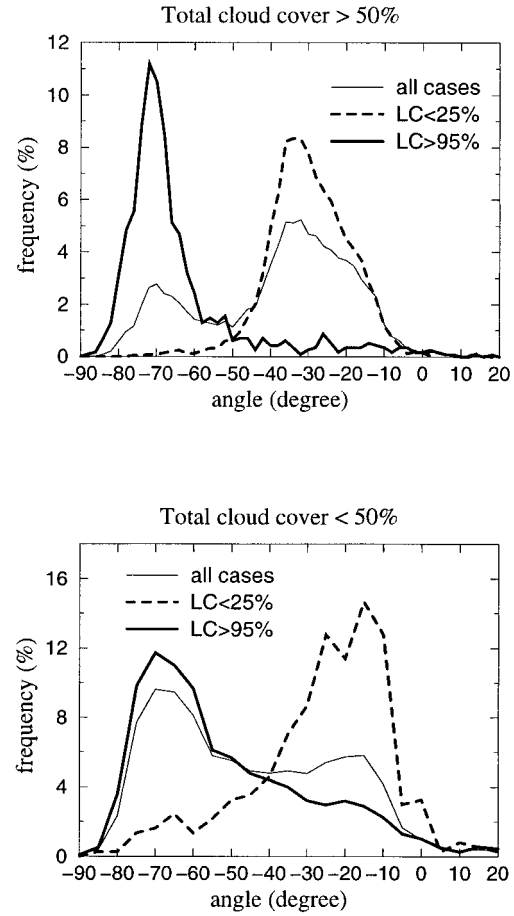

FIG. 4. Distribution of the Θ values of the INSAT VIS–IR scatterplot diagrams obtained in each 2.5° × 2.5° ocean region within two bands of longitude (45°–55°E and 85°–95°E) between 35°S and 25°N during Feb 1986–89. Fine solid line is the distribution obtained by considering all regions for which the cloud AWP is larger (top) or smaller (bottom) than 50%. Thick lines represent distributions obtained by considering only the regions that are classified by ISCCP/C1 as cloudy and covered by less than 25% (dashed line) or more than 95% (solid line) of low-level clouds.

[3] Note that to minimize sun-angle effects in the spatial variability of visible radiances and to exclude terminator situations, we ignore regions of the Indian Ocean for which the cosine of the solar zenith angle is less than 0.3. This value is similar to that used in ISCCP to distinguish day/night situations (Rossow et al. 1996).

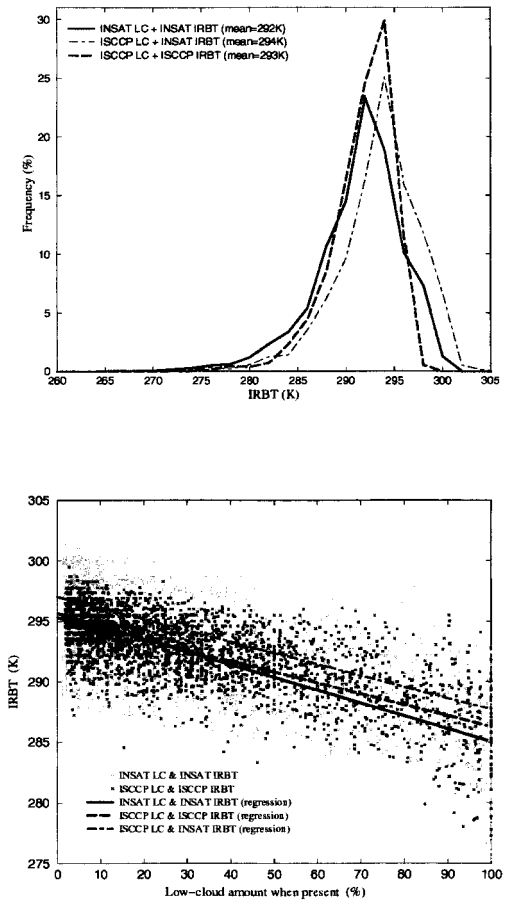

FIG. 5. (a) Distribution of the 2.5° × 2.5° mean IRBT values derived from INSAT or ISCCP/C1 data in regions classified as covered by low-level clouds only (LC) by INSAT or by ISCCP/C1. Comparison between solid and dot–dashed lines shows the impact of cloud classification differences between INSAT and ISCCP/C1, while comparison between dot–dashed and dashed lines shows the impact of IR radiances differences. (b) 2.5° × 2.5° IRBT vs the 2.5° × 2.5° cloud amount when present derived from INSAT (dot markers and solid regression line) or ISCCP/C1 (cross markers and dashed regressions line). Also reported (dot–dashed line) is the regression line obtained using ISCCP low-cloud classification and coincident INSAT IRBT. Those figures are based on data ranging from 35°S to 25°N in two different bands of longitudes (45°–55°E and 85°–95°E) during Feb 1986–89.

Meteosat, GMS, or AVHRR) radiances. This might indicate a systematic bias in the absolute calibration of INSAT IR radiances. As a result, the IRBT–AWP relationship derived from INSAT is very close from that derived from ISCCP, but this results from compensatory effects: a systematic overestimate of INSAT IRBT related to calibration, and an underestimate of the INSAT IRBT from low-level clouds of higher top altitude than identified by the ISCCP algorithm.

Comparison against ISCCP suggests that our simple methodology for identifying nonoverlapped low clouds yields cloud systems with similar radiative characteristics. This is the primary justification for using our analysis procedure as a complementary approach to investigate the geographical and seasonal variations of low-level clouds over the Indian Ocean.

4. Low-cloud occurrence and amount when present

The monthly frequency of occurrence of nonoverlapped low clouds during January–April has been derived from INSAT data (Fig. 6), ISCCP/C1 data (Fig. 7), and surface observations (Fig. 8). The three datasets indicate that NOLC occur on both sides of the ITCZ, mostly over the southern Indian Ocean southward of about 15°S, and over the Arabian Sea, the Bay of Bengal, and the China Sea northward of about 5°N. The occurrence is much weaker at equatorial latitudes. Since upper-level cloudiness is greatest in the ITCZ, the decrease in NOLC frequency at these latitudes may reflect the lower probability of detecting low clouds near or underneath upper-level cloud systems.

While marine low clouds occur over most subtropical regions, we observe large gradients in the amount when present (Figs. 6, 7, and 8, lower panels). In particular, clouds covering the Arabian Sea and the Bay of Bengal appear to be more broken with lower values of AWP than over the southern Indian Ocean and South China Sea. These gradients will be discussed in more detail in section 5.

The occurrence of NOLC exhibits some seasonal evolution from January to April. Over the Arabian Sea, the occurrence decreases with time and the maximum of the distribution moves slightly southward. INSAT data indicate a rapid decrease in NOLC between March and April. This trend is also present to a lesser degree in the ISCCP and surface observations. A similar decrease is observed over the China Sea. Over the southern Indian Ocean, a strong maximum in NOLC is seen in January–February. In March a second maximum appears around 70°E, and the distribution becomes more uniform southward of about 25°S in April. The dataset of Hahn et al. (1996) has been analyzed to determine if changes in the monthly frequency of upper level clouds could explain part of the trends found in NOLC. The average change in upper-level cloud have been computed from January to February and from March to April. The results suggest the rapid decrease in NOLC between March and April in the Arabian Sea is largely explained by the rapid increase in upper-level cloudiness (not shown).

Besides these main features in the distribution of NOLC, some discrepancies in the frequency of NOLC are apparent among the three datasets. Comparison of satellite and surface observations for exactly the same time period (1986–89) leads to similar discrepancies. Over the whole of the Indian Ocean sector, surface observations report higher frequencies of nonoverlapped low clouds than INSAT or ISCCP data. One explanation is related to the difference in spatial scales of the surface and satellite observations. The satellite methods as for-

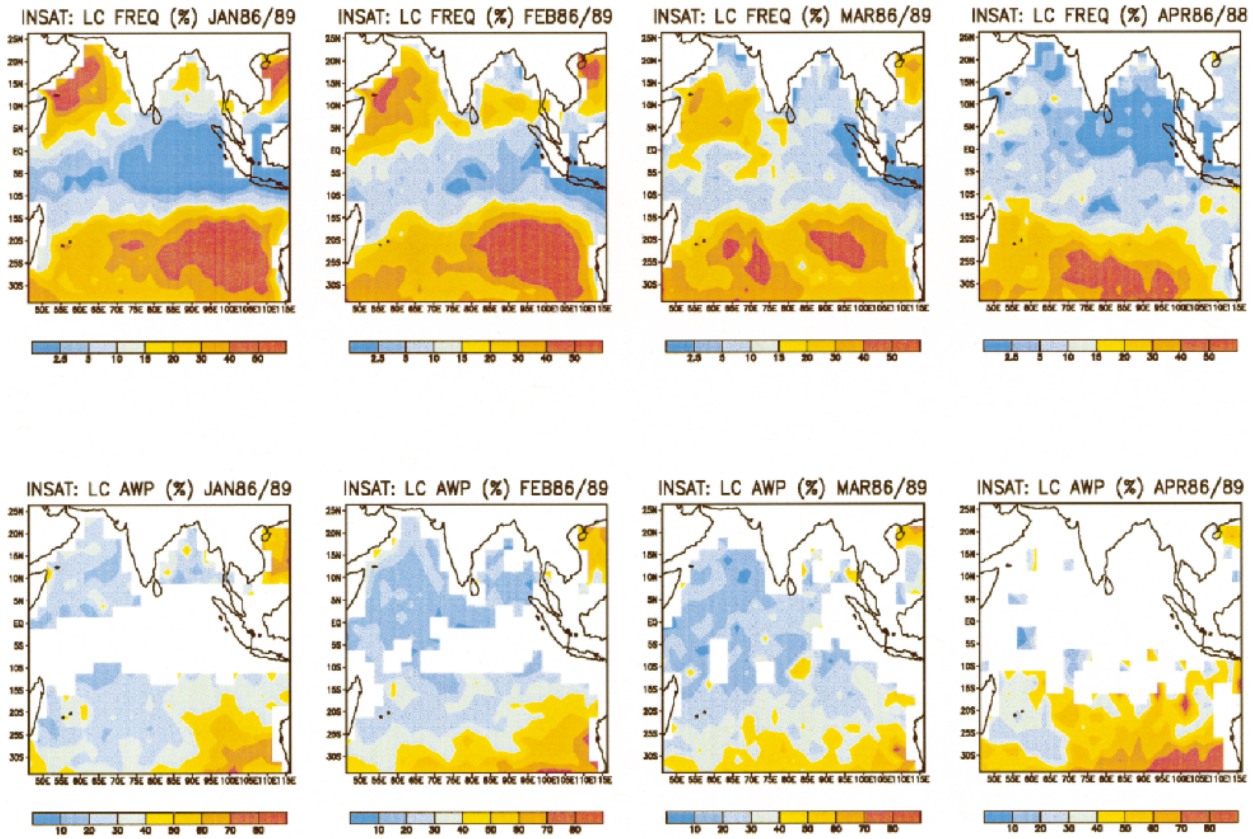

FIG. 6. Monthly frequency of occurrence (top) and amount when present (bottom) of nonoverlapped low clouds derived from INSAT data during 1986–89 from 0600 to 0900 UTC at a resolution 2.5° × 2.5° (AWP values are not displayed in regions where the monthly frequency of occurrence is less than 5%). Units: %.

mulated here require that there is no detectable mid- or upper-level cloud within a 2.5° region. The ship observations of low clouds are counted as NOLC if no mid- or upper-level cloud is present within the field of view (FOV) of the surface observer. The radius of this FOV is typically much smaller than the satellite analysis grid, thereby reducing the probability of cloud contamination by mid- and upper-level systems. The higher NOLC frequencies from surface data may be due also to the difficulty of detecting from a surface platform whether extensive low-cloud systems are overlapped by upper-level clouds. These two factors can explain at least part of the systematic difference between surface and satellite frequencies.

Discrepancies are found also between the two satellite datasets. As explained in section 3c, the criteria used to identify low clouds from INSAT data allow colder cloud tops than the ISCCP/C1 criteria, especially for large cloud amounts. Therefore in regions where cumulus clouds exhibit a spectrum of cloud tops, the INSAT-derived frequency of occurrence of NOLC will be equal to, or larger than, that derived from ISCCP. However over the Bay of Bengal and the Arabian Sea where the AWP is weak, the INSAT algorithm yields lower frequencies of occurrence of low-cloud systems than ISCCP. The sensitivity of the two satellite detection algorithms to the presence of partial or broken cloudiness is different for several reasons, including the fact that the viewing angles of the GMS and Meteosat satellites over those regions are much larger than those of INSAT. However, as discussed in the previous section, this regional discrepancy between INSAT and ISCCP results may also be related to the choice of Θ_0 for AWP <50%. Indeed, sensitivity experiments indicate that this discrepancy is greatly reduced when using a lower Θ_0 ($-30°$ for instance) for AWP <50%. Nevertheless, the amount when present of those clouds is very small in those regions (Figs. 6–8, lower panels). Therefore the absolute difference in the average low-cloud amount (which may be computed as the frequency of occurrence times the amount when present) between the two datasets is also small.

5. Consistency with meteorological conditions

INSAT, ISCCP/C1, and surface data all show that low clouds mainly occur at subtropical latitudes, exhibit some seasonal variation between January and April, and have larger AWP in the Southern Hemisphere. The consistency of those features with the meteorological con-

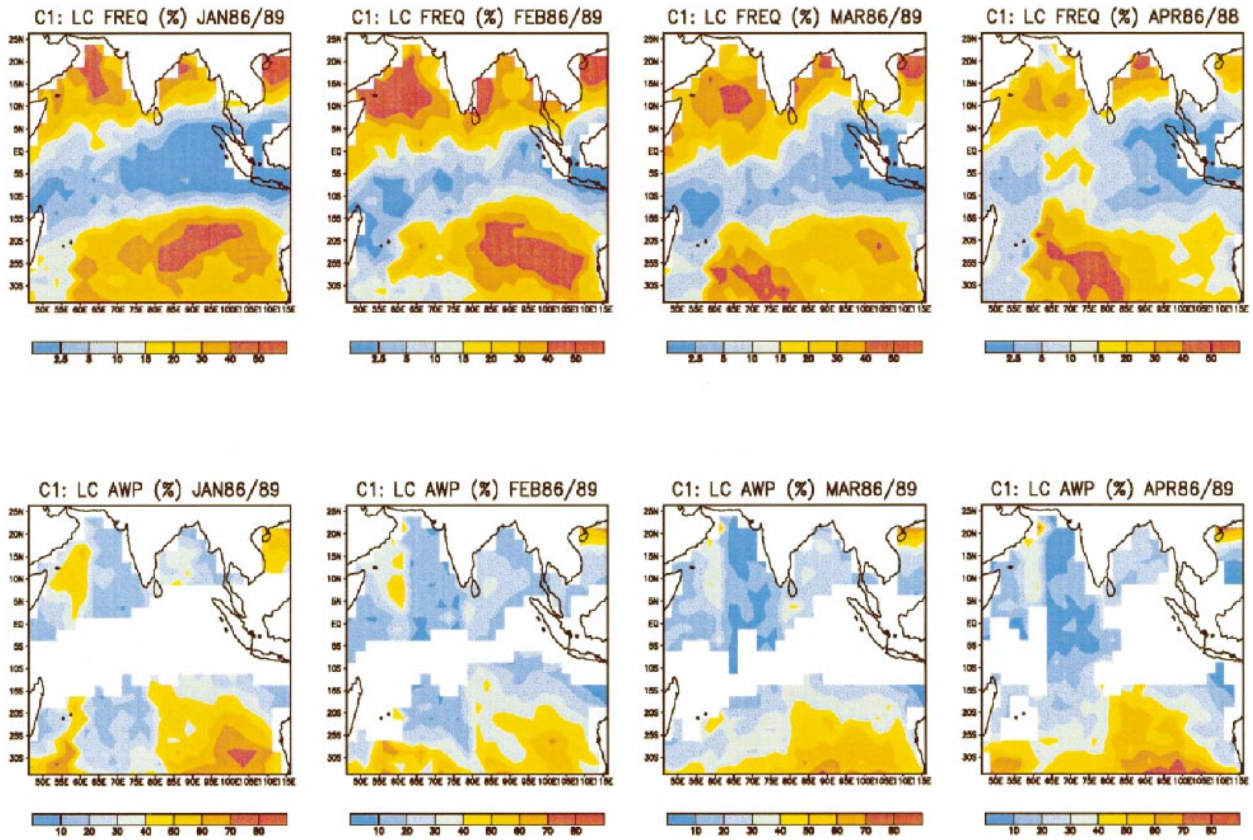

FIG. 7. Monthly frequency of occurrence (top) and amount when present (bottom) of nonoverlapped low clouds derived from ISCCP/C1 data during 1986–89 at 0600 and 0900 UTC (AWP values are not displayed in regions where the monthly frequency of occurrence is less than 5%). Units: %.

ditions over the Indian Ocean can be evaluated with the daily ECMWF reanalysis (ERA; Gibson et al. 1997) for the period January–April 1986–89. The quality of ERA over the Indian Ocean is presumably affected by the sparsity of the in situ data available for the analysis. Nevertheless, we can reasonably assume that the main large-scale meteorological features of this region are represented with some fidelity. This analysis will not address the physics of low-level clouds or document the meteorological conditions required for the formation of NOLC. The objective is to assess the consistency of the distributions of NOLC with meteorological conditions favorable to the formation of low-level clouds based upon studies of other oceanic regions (Klein 1997; Norris 1998a).

Nonoverlapped low clouds are expected to occur in regions of large-scale subsidence, where the adiabatic warming of the subsiding atmosphere produces an atmospheric temperature inversion and a stable troposphere. Several observational studies show that on the monthly timescale, low-cloud amount is well correlated to several meteorological parameters such as the sea surface temperature and the static stability of the lower troposphere (e.g., Hanson 1991; Klein and Hartmann 1993; Norris 1998a). We recognize that the conditions of formation of NOLC may not be identical to those of low clouds in general, and that these conditions may differ also from one region of the globe to another. Nevertheless, as for low clouds in general, the conditions of formation of NOLC over the Indian Ocean are presumably related to a large static stability of the atmosphere and to the presence of atmospheric inversions. The goal of the present analysis is to check the consistency between the NOLC statistics presented above and the meteorological conditions of the Indian Ocean as represented in the ERA.

In this study, the static stability S is defined as the difference between the potential temperature at 700 hPa and at the surface. Temperature inversions are reported in regions where the saturation equivalent potential temperature Θ_e^* increases with height (Emanuel 1994). The strength of the inversions is characterized with the following index:

$$\frac{\displaystyle\int_{\text{base}}^{\text{top}} \frac{d\Theta_e^*(z)}{dz}\rho\, dz}{\displaystyle\int_{\text{base}}^{\text{top}} \rho\, dz}, \tag{1}$$

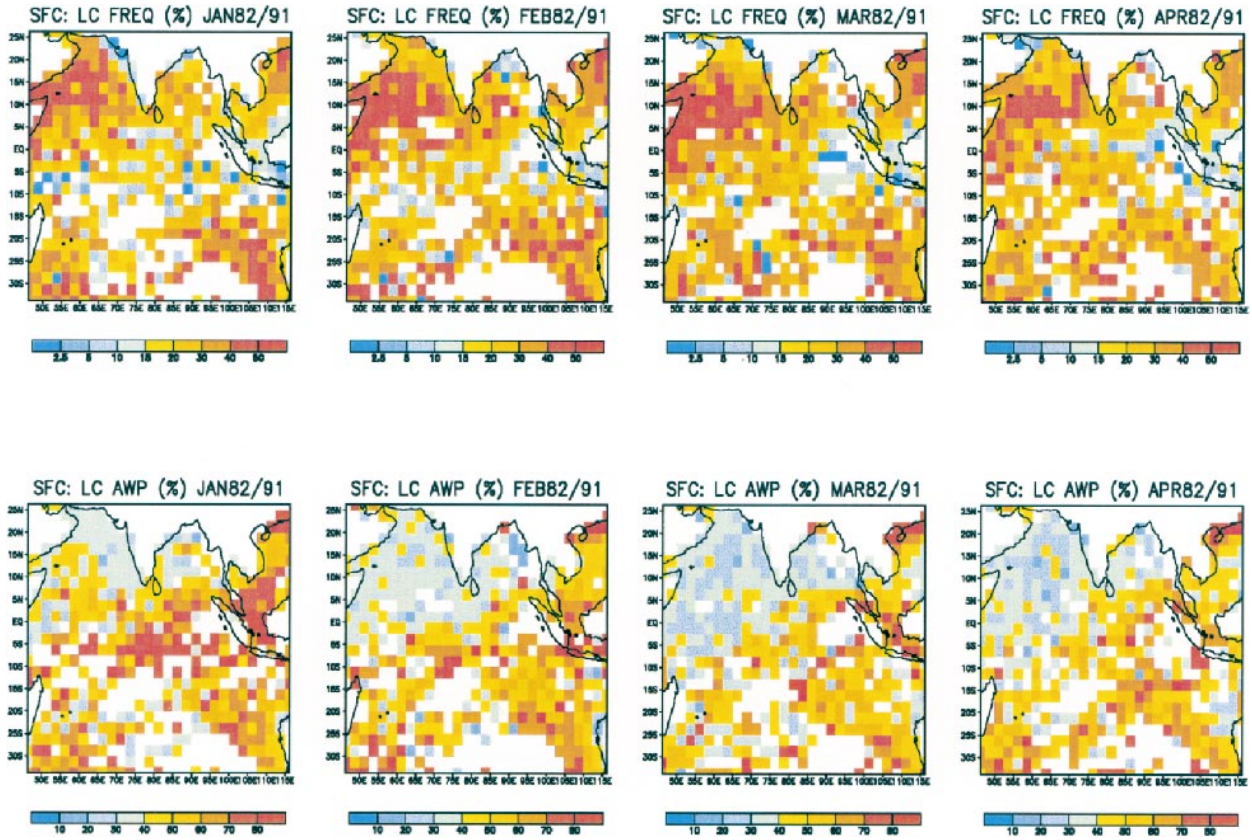

FIG. 8. Monthly frequency of occurrence (top) and amount when present (bottom) of nonoverlapped low clouds derived from surface observations compiled by Hahn–Warren–London for 1982–91 for 0600–0900 UTC (AWP values are not displayed in regions where the monthly frequency of occurrence is less than 5%). Units: %.

where the integration extends from the lower (base) to the upper (top) limits of the inversion. The base (top) of the inversion is defined here as the lowest ERA level above the surface layer where Θ_e^* starts increasing (decreasing). The vertical resolution of the ERA data used in this study is 75 mb. The sensitivity of the inversion frequency and inversion strength to vertical resolution has been tested using radiosonde profiles over the Indian Ocean.[4] The profiles are from the National Centers for Environmental Prediction global upper-air database and include all available observations for 1985–94. The data have been analyzed for four sectors covering the northeast, northwest, southeast, and southwest corners of the Indian Ocean. The temperature and humidity have been interpolated onto vertical grids with variable spacing, and then the inversion frequency and strength have been computed from the interpolated data. The results indicate that these parameters are not very sensitive to vertical resolution unless the spacing of the grid exceeds 50 mb (not shown). The ratio of the frequencies and strengths evaluated with vertical resolutions of 75 and 10 mb is shown in Table 1. For a spacing of 75 mb, both the strength and frequency of the inversions are underestimated, with the largest underestimate occurring in the inversion strength.

Over the Indian Ocean, the occurrence of low-level clouds shown on Figs. 6–8 is positively correlated with the lower tropospheric stability and with the strength of atmospheric inversions (Fig. 9). It also appears to be highly correlated with the frequency of occurrence of inversions, which are usually expected to cap nonoverlapped low clouds in subtropical regions.

In the Northern Hemisphere, INSAT data indicate a strong seasonal variation of the low-cloud occurrence

TABLE 1. The ratio of inversion frequency and inversion strength evaluated by interpolating ship radiosonde profiles of T and q onto vertical grids with 75- and 10-mb resolution. The resolution of 75 mb is identical to the resolution of the ERA in the lower troposphere used for this analysis. The quantity evaluated at 10-mb resolution is in the denominator. The ratios have been computed for four quadrants in the Indian Ocean: 0°–30°N, 75°–105°E (NE); 0°–30°N, 45°–75°E (NW); 30°S–0°, 75°–105°E (SE); and 30°S–0°, 45°–75°E (SW).

Ratio	NE	NW	SE	SW
Inversion frequency	0.72	0.85	0.56	0.96
Inversion strength	0.47	0.44	0.37	0.47

[4] Unfortunately, the ship radiosonde data are too sparse to permit derivation of maps of the inversions directly from in situ data.

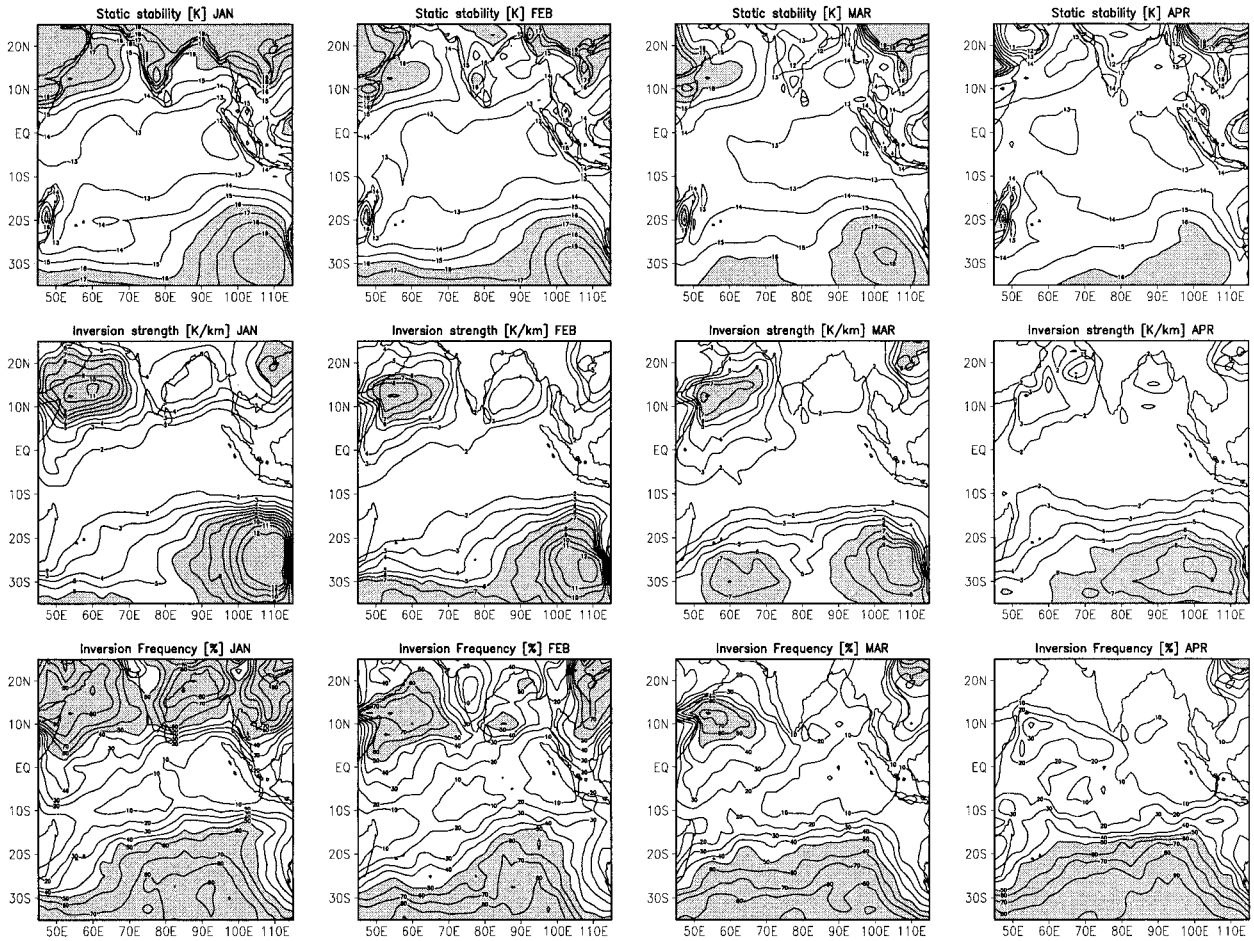

FIG. 9. Meteorological parameters derived from daily ERA for Jan–Apr 1986–89: (top) the static stability (middle) an index related to the strength of atmospheric inversions and (bottom) the frequency of occurrence of atmospheric inversions.

(section 4). The progressive dissipation of low clouds during Northern Hemisphere spring is particularly evident between March and April over the Arabian Sea and between February and March over the Bay of Bengal. The decrease in NOLC is closely related to the decrease in static stability of the lower troposphere and to the decrease in the frequency of occurrence of atmospheric inversions. The largest increases in sea surface temperature (SST) are coincident with the sharpest decreases in the low-cloud amount (Fig. 10). Over the Arabian Sea, the southward shift with time of the maximum in low clouds is consistent with coincident changes in the occurrence of temperature inversions. Over the southern Indian Ocean, the eastward shift of the low-cloud maximum between March and April is consistent with the eastward displacement of the high-pressure center (not shown) and with changes in static stability (Fig. 9). But the displacement appears to be correlated primarily with changes in both the frequency and the intensity of atmospheric inversions.

The correlation between meteorological parameters and the NOLC frequency for four selected areas is displayed on Fig. 11. In all three regions of the Northern Hemisphere, the progressive decrease of low-cloud frequency from January to April is associated with a warming of the surface ocean, and with a decrease of the static stability of the atmosphere and of the frequency and strength of atmospheric inversions. In the Southern Hemisphere, the static stability exhibits some seasonal variation, while the SST and the atmospheric inversions (frequency and strength) vary much less than in the Northern Hemisphere. In this region, the seasonal variation of NOLC seems to be better related to changes in atmospheric inversions than to changes in the static stability. In all four regions, the seasonal variation of NOLC appears to be consistent with that of surrounding meteorological conditions.

Recent observational studies have yielded relationships between low-cloud type, the meteorology of the marine boundary layer (MBL), and surface conditions (e.g., Albrecht et al. 1995; Klein 1997; Norris 1998a). Depending on the SST and on the vertical structure of

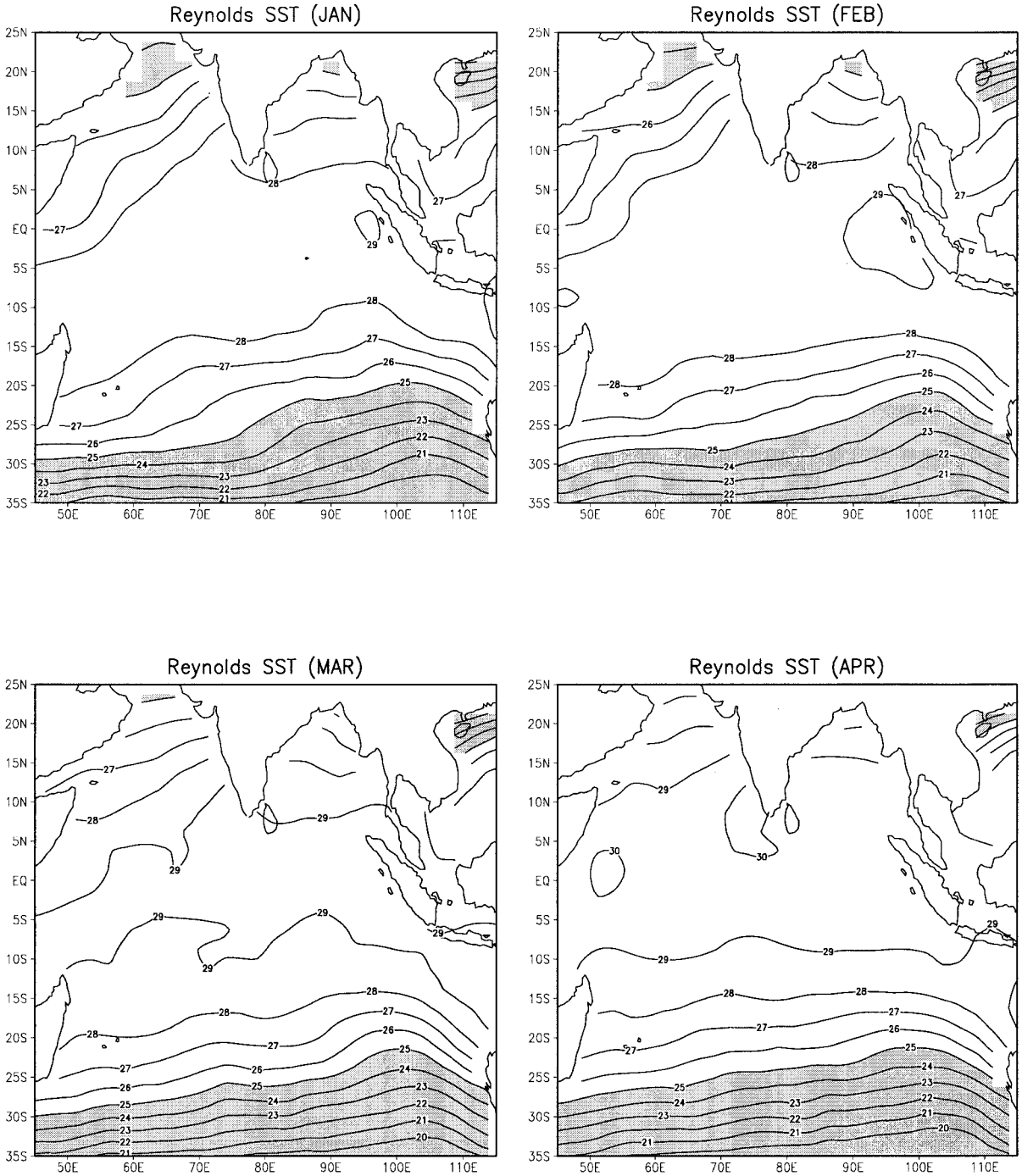

FIG. 10. Monthly mean sea surface temperature (°C) for Jan–Apr 1986–89 derived from Reynolds (1988) data.

the MBL and free troposphere, the primary morphology of low-cloud systems can be stratocumulus, cumulus rising into stratocumulus, or cumulus. The transition between stratocumulus and cumulus regimes is related to the decoupling of the MBL characterized by the vertical gradient of humidity within the subcloud layer. As shown by Norris (1998a), the degree of MBL decoupling can be characterized by the parameter

$$\Delta q = 100 \times \frac{[q(z/z_i = 0.2) - q(z/z_i = 0.9)]}{q_s(\mathrm{SST})},$$

where q is the specific humidity, $q_s(\mathrm{SST})$ is the saturation specific humidity at the sea surface, and z_i the height of the MBL. The MBL height is defined here as the base height of the capping inversion, that is, Θ_e^* increasing with height. The parameter Δq has been de-

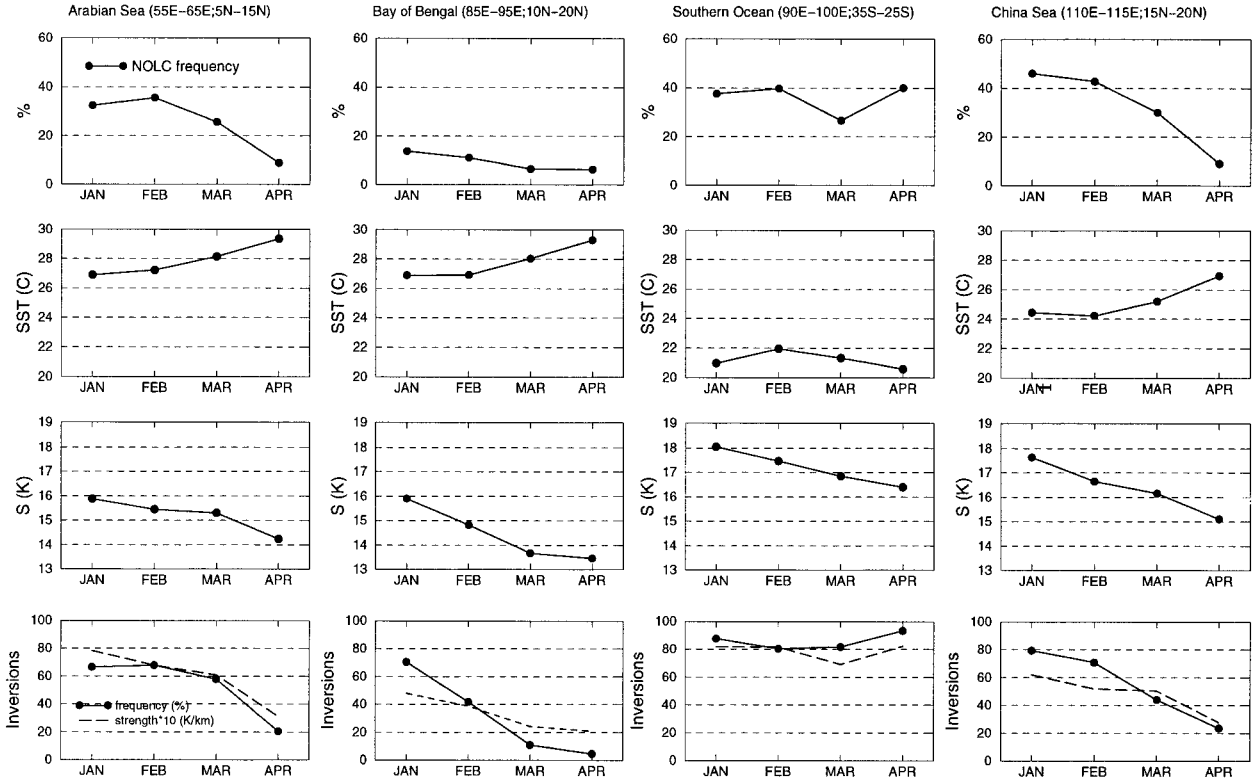

FIG. 11. Monthly mean NOLC frequency, SST, static stability *S*, and the frequency and strength of inversions for four regions of the Indian Ocean and China Sea.

rived from daily ERA fields. Note that the accuracy of this parameter is affected by the coarse vertical resolution of ERA in the MBL and by the limited amount of radiosonde data assimilated in the analysis procedure. Thus the values of Δq from the ERA provide only qualitative information about the large-scale spatial and seasonal variations of the MBL decoupling. Results indicate that the values of the decoupling parameter are generally inversely related to the AWP (not shown).

Previous studies have pointed out systematic relationships between low-cloud types, meteorological conditions and AWP. Over the Arabian Sea and the Bay of Bengal, SSTs range between 24° and 28°C in January–February, 25° and 29°C in March, and 27° and 30°C in April (Fig. 10). The static stability ranges between 13° and 17°C (Fig. 9). The large values of the decoupling parameter from the ERA (not shown) suggest that the MBL is somewhat decoupled and the AWP is generally lower than 50% (Figs. 6–8). Assuming that the meteorological conditions associated with the formation of NOLC may be different, but not drastically different, from those of low clouds in general, previous studies (Albrecht et al. 1995; Klein 1997; Norris 1998a,b) suggest that the NOLC forming in those regions are mostly of cumulus type.

Over the southern Indian Ocean and the China Sea, the SST is generally less than 25°C; the lower troposphere is much more stable than over the Arabian sea or the Bay of Bengal; and the MBL is less decoupled. These conditions, together with the higher amounts when present of low clouds (40%–80%), suggest that the low-level clouds are mostly stratocumulus. These results, which were derived from combining satellite data and meteorological analyses, confirm that results from previous studies based on ship and surface observations (Warren et al. 1988; Norris 1998a,b) are applicable over large areas of the Indian Ocean region.

6. Summary and conclusions

This paper is an analysis of the occurrence of nonoverlapped low cloud systems over the Indian Ocean and South China Sea during the winter monsoon (January–April). Climatologies from the ISCCP/C1 dataset and from surface synoptic reports are presented, and a complementary investigation is performed with data from the Indian geostationary satellite (INSAT). The INSAT data are processed using a simple detection method for low clouds based on the relative mesoscale spatial variability of the infrared and visible radiances. The advantage of the new dataset relative to ship observations is the much higher spatial and temporal resolution. The higher resolution permits analysis of the relationships between NOLC and other remotely sensed datasets. The advantage of the new dataset relative to ISCCP is that the characterization of NOLC is based

upon geosynchronous satellite imagery obtained directly over the regions of interest.

The distributions of NOLC obtained from the three datasets are generally in good agreement. During daytime, regions covered by low clouds occur mainly over the Arabian Sea, the Bay of Bengal, the China Sea northward of about 5°N, and the southern Indian Ocean southward of about 15°S. However, the amount when present of low clouds is much lower in the Northern Hemisphere than in the Southern Hemisphere. The gradient in AWP and inspection of coincident surface and meteorological analyses show that low clouds are cumulus over the Arabian Sea and the Bay of Bengal. The NOLC are mostly stratocumulus over the southern Indian Ocean.

There is a sharp decrease in the occurrence of nonoverlapped cumulus clouds between March and April over the Arabian Sea and between February and March over the Bay of Bengal. Examination of the surface and meteorological conditions shows that this is coincident with the warming of the ocean, the decrease in tropospheric stability, and the increase in the frequency of upper-altitude clouds. In the Southern Hemisphere, the seasonal variation of the low-cloud occurrence is correlated with changes in the frequency and intensity of atmospheric inversions.

The Indian Ocean is surrounded by nations that are becoming increasingly significant sources of anthropogenic aerosols. During the winter monsoon, the large-scale atmospheric circulation transports aerosols from the Indian subcontinent toward ocean regions that we have shown to be covered primarily by cumulus clouds. Subsequent papers will analyze the physical, microphysical, and radiative properties of the low clouds of the Indian Ocean, taking advantage in particular of the data collected during the Indian Ocean Experiment (Ramanathan et al. 1996). A primary goal of these subsequent investigations will be to quantify the indirect effect of aerosols using observations of aerosol optical depth, liquid water path, and cloud albedo at the top of the atmosphere. Depending on this indirect effect, the cumulus clouds of the northern Indian Ocean may play an important role in regional climate change.

Acknowledgments. The authors acknowledge the National Center for Atmospheric Research and the Indian Meteorological Department for providing INSAT data. This study started when the first author visited the Center for Clouds, Chemistry and Climate of the Scripps Institution of Oceanography at the invitation of V. Ramanathan. The first author is particularly grateful to G. Sèze (LMD), who provided judicious advice and comments during the course of this study. The authors also thank J. Norris (NCAR) for many useful comments and discussions. Two anonymous reviewers made many constructive recommendations for improving the manuscript. SB was supported in part by the French ''Mesoscale Atmosphere and Ocean Program'' (PATOM) and WDC was supported in part by NASA MTPE Grant S-97889-F. This is C4 INDOEX Publication 29.

REFERENCES

Albrecht, B. A., M. P. Jensen, and W. J. Syrett, 1995: Marine boundary layer structure and fractional cloudiness. *J. Geophys. Res.,* **100** (D7), 14 209–14 222.

Arking, A., and J. D. Childs, 1985: Retrieval of cloud cover parameters from multispectral satellite measurements. *J. Climate Appl. Meteor.,* **24,** 322–333.

Cahalan, R. F., W. Ridgway, W. J. Wiscombe, T. L. Bell, and J. B. Snider, 1994: The albedo of fractal stratocumulus clouds. *J. Atmos. Sci.,* **51,** 2434–2455.

Coakley, J. A., Jr., and D. G. Baldwin, 1984: Towards the objective analysis of clouds from satellite imagery data. *J. Climate Appl. Meteor.,* **23,** 1065–1099.

Desbois, M., and G. Sèze, 1984: Application of the clustering method for the cloud cover analysis over tropical regions. *Proc. ECMWF Workshop on Cloud Cover Parameterization in Numerical Models,* Reading, United Kingdom, ECMWF, 263–283.

Desormeaux, Y., W. B. Rossow, C. L. Brest, and G. G. Campbell, 1993: Normalization and calibration of geostationary satellite radiances for the International Satellite Cloud Climatology Project. *J. Atmos. Oceanic Technol.,* **10,** 304–325.

Emanuel, K. A., 1994: *Atmospheric Convection.* Oxford University Press, 580 pp.

Gibson, J. K., P. Kallberg, S. Uppala, A. Nomura, A. Hernandez, and E. Serrano, 1997: ERA description. ECMWF Re-Analysis Project Report Series 1, ECMWF, Reading, United Kingdom, 72 pp.

Hahn, C. J., S. G. Warren, and J. London, 1996: Edited synoptic cloud reports from ships and land stations over the globe, 1982–1991. Tech. Rep. NDP026B, Carbon Dioxide Information Analysis Center, Oak Ridge National Laboratory, Oak Ridge, TN, 45 pp. [Available from Carbon Dioxide Information Analysis Center, Oak Ridge National Laboratory, P.O. Box 2008, Oak Ridge, TN 37831-6335.]

Hanson, H. P., 1991: Marine stratocumulus climatologies. *Int. J. Climatol.,* **11,** 147–164.

Hartmann, D. L., M. E. Ockert-Bell, and M. L. Michelsen, 1992: The effect of cloud type on the earth's energy balance: Global analysis. *J. Climate,* **5,** 1281–1304.

Klein, S. A., 1997: Synoptic variability of low-cloud properties and meteorological parameters in the subtropical trade wind boundary layer. *J. Climate,* **10,** 2018–2039.

——, and D. L. Hartmann, 1993: The seasonal cycle of low stratiform clouds. *J. Climate,* **6,** 1587–1606.

Krishnamurti, T. N., B. Jha, P. J. Rasch, and V. Ramanathan, 1997a: A high resolution global reanalysis highlighting the winter monsoon. Part 1: Reanalysis fields. *Meteor. Atmos. Phys.,* **64** (3–4), 123–150.

——, ——, ——, and ——, 1997b: A high resolution global reanalysis highlighting the winter monsoon. Part 2: Transients and passive tracer transports. *Meteor. Atmos. Phys.,* **64** (3–4), 151–171.

Mechoso, C., and Coauthors, 1995: The seasonal cycle over the tropical Pacific in coupled ocean–atmosphere general circulation models. *Mon. Wea. Rev.,* **123,** 2825–2838.

Norris, J. R., 1998a: Low cloud type over the ocean from surface observations. Part I: Relationship to surface meteorology and the vertical distribution of temperature and moisture. *J. Climate,* **11,** 369–382.

——, 1998b: Low cloud type over the ocean from surface observations. Part II: Geographical and seasonal variations. *J. Climate,* **11,** 383–403.

Platt, C. M. R., 1983: On the bispectral method of cloud parameter determination from satellite VISSR data: Separating broken

cloud and semi-transparent cloud. *J. Climate Appl. Meteor.*, **22,** 429–439.

Ramanathan, V., and Coauthors, 1996: INDOEX: A multi-agency proposal for a field experiment in the Indian Ocean. Scripps Institution of Oceanography Internal Rep., 82 pp. [Available from C4/SIO, La Jolla, CA 92093-0239.]

Reynolds, R. W., 1988: A real-time global sea surface temperature analysis. *J. Climate,* **1,** 75–86.

Rossow, W. B., and R. A. Schiffer, 1991: ISCCP cloud data products. *Bull. Amer. Meteor. Soc.,* **72,** 2–20.

——, and L. C. Garder, 1993: Validation of ISCCP cloud detections. *J. Climate,* **6,** 2370–2393.

——, ——, P.-J. Lu, and A. Walker, 1991: International Satellite Cloud Climatology Project (ISCCP): Documentation of cloud data. WMO/TD-No. 266, WCRP, Geneva, Switzerland, 122 pp.

——, Y. Desormeaux, C. L. Brest, and A. Walker, 1992: International Satellite Cloud Climatology Project (ISCCP). Radiance calibration report. WMO/TD No. 520, WCRP, Geneva, Switzerland, 104 pp.

——, A. W. Walker, D. E. Beuschel, and M. D. Roiter, 1996: International Satellite Cloud Climatology Project (ISCCP): Documentation of new cloud datasets. WMO/TD-No. 737, WCRP, Geneva, Switzerland, 115 pp.

Schwarz, S. E., and A. Slingo, 1996: Enhanced shortwave cloud radiative forcing due to anthropogenic aerosols. *Clouds, Chemistry and Climate,* P. J. Crutzen and V. Ramanathan, Eds., NATO ASI Series I, Vol. 35, Springer-Verlag 191–236.

Sèze, G., and W. B. Rossow, 1991: Time-cumulated visible and infrared radiance histograms used as descriptors of surface and cloud variations. *Int. J. Remote Sens.,* **12,** 877–920.

Smith, E. A., K. W. Oh, and M. R. Smith, 1989: A PC-based interactive imaging system designed for INSAT data analysis and monsoon studies. *Bull. Amer. Meteor. Soc.,* **70,** 1105–1122.

Tiernego, R., 1996: Calibration of the INSAT-1B satellite with NOAA-11 AVHRR data. Scripps Institution of Oceanography internal report, 27 pp. [Available from C4/SIO, La Jolla, CA 92093-0239.]

Warren, S. G., C. J. Hahn, J. London, R. M. Chervin, and R. L. Jenne, 1988: Global distribution of total cloud cover and cloud type amounts over the ocean. NCAR Tech. Note NCAR/TN-317+STR, NCAR, Boulder, CO, 212 pp.

Wolf, M., and G. M. Hidy, 1997: Aerosols and climate: Anthropogenic emissions and trends for 50 years. *J. Geophys. Res.,* **102,** 11 113–11 121.